

Near-Optimal Low-Complexity MIMO Detection via Structured Reduced-Search Enumeration

Logeshwaran Vijayan

Abstract—Maximum-likelihood (ML) detection in high-order MIMO systems is computationally prohibitive due to exponential complexity in the number of transmit layers and constellation size. In this white paper, we demonstrate that for practical MIMO dimensions (up to 8×8) and modulation orders, near-ML hard-decision performance can be achieved using a structured reduced-search strategy with complexity linear in constellation size. Extensive simulations over i.i.d. Rayleigh fading channels show that list sizes of $3|\mathcal{X}|$ for 3×3 , $4|\mathcal{X}|$ for 4×4 , and $8|\mathcal{X}|$ for 8×8 systems closely match full ML performance, even under high channel condition numbers, $|\mathcal{X}|$ being the constellation size. In addition, we provide a trellis based interpretation of the method. We further discuss implications for soft LLR generation and FEC interaction.

Index Terms—MIMO, Maximum-likelihood (ML), Trellis, Soft-llrs, Sphere Decoder, FEC, ZF, QR, SU-MIMO, MU-MIMO.

I. INTRODUCTION

MIMO detection remains a fundamental challenge in modern wireless systems due to the exponential growth of the ML search space: $|\mathcal{X}|^{N_t}$, where N_t is the number of transmit layers and $|\mathcal{X}|$ is the constellation size.

While sphere decoding and lattice-reduction techniques reduce average complexity, worst-case behavior remains prohibitive for hardware implementation. This motivates structured reduced-search detectors that exploit channel geometry, ordering, and diversity properties.

This work builds on that motivation and demonstrates that *exact ML hard decisions* can often be recovered using dramatically smaller candidate lists.

II. SYSTEM MODEL

We consider a narrowband flat-fading MIMO system:

$$\mathbf{y} = \mathbf{H}\mathbf{x} + \mathbf{n}, \quad (1)$$

where $\mathbf{H} \in \mathbb{C}^{N_r \times N_t}$ is the channel matrix, $\mathbf{x} \in \mathcal{X}^{N_t}$ is the transmit vector and $\mathbf{n} \sim \mathcal{CN}(0, \sigma^2 \mathbf{I})$.

Applying QR decomposition (with possible column permutation \mathbf{P}),

$$\mathbf{H}\mathbf{P} = \mathbf{Q}\mathbf{R}, \quad (2)$$

where \mathbf{Q} is unitary and \mathbf{R} is upper triangular. Left-multiplying by \mathbf{Q}^H gives

$$\tilde{\mathbf{y}} = \mathbf{R}\tilde{\mathbf{x}} + \tilde{\mathbf{n}}, \quad (3)$$

The algorithm behind this paper was originally invented/implemented, applied for patent and granted in 2005, 2007 and 2011 respectively while the author was with Redpine Signals Inc., which was later acquired by Silicon Labs. However, this paper does an independent analysis of it.

with

$$\tilde{\mathbf{y}} = \mathbf{Q}^H \mathbf{y}, \quad \tilde{\mathbf{x}} = \mathbf{P}^T \mathbf{x}, \quad \tilde{\mathbf{n}} = \mathbf{Q}^H \mathbf{n}.$$

Expanding above equation,

$$\tilde{y}_i = \sum_{j=i}^{N_t} r_{ij} x_j + \tilde{n}_i, \quad i = 1, \dots, N_t, \quad (4)$$

which is directly analogous to a causal ISI channel with memory $N_t - i$.

Maximum-likelihood detection therefore corresponds to minimizing the global metric

$$\hat{\mathbf{x}} = \arg \min_{\mathbf{x} \in \mathcal{S}^{N_t}} \sum_{i=1}^{N_t} \left| \tilde{y}_i - \sum_{j=i}^{N_t} r_{ij} x_j \right|^2, \quad (5)$$

III. PROPOSED DETECTOR

The main idea behind this paper was applied for patent in 2007 and granted in 2011 [1]. To the best of author's knowledge, there is a similar/closely related method that was proposed around the same time-frame by another set of authors [2]. In this paper, we provide a different interpretation/explanation of the method. In that sense, this work represents an independent theoretical analysis. The results are based on computer simulations of publicly disclosed algorithmic principles [1], [2] and do not represent the proprietary implementation of any specific commercial product. To accurately reflect its operational characteristics, we refer to this detector as the *Multi-Pivot Multiple-Hypothesis Trellis-Like MIMO Detector (MP-MHT-MD)*.

The detector interprets the QR-transformed MIMO system as a spatial ISI channel and performs a depth-wise hypothesis search analogous to a trellis decoder. Unlike conventional sphere decoding, which prunes paths early based on partial metrics from a single pivot layer, the proposed method cyclically enumerates each spatial layer as a pivot and preserves multiple competing hypotheses until sufficient decoding depth is reached. This delayed-pruning strategy ensures that near-ML paths are not prematurely eliminated, resulting in ML-equivalent hard decisions with drastically reduced search complexity.

We explain the algorithm here for 3×3 MIMO system.

$$y_3 = r_{33}x_3 + n_3 \quad (6)$$

$$y_2 = r_{22}x_2 + r_{23}x_3 + n_2 \quad (7)$$

$$y_1 = r_{11}x_1 + r_{12}x_2 + r_{13}x_3 + n_1 \quad (8)$$

We pivot on x_3 and search over all possible hypothesis. For each hypothesis of x_3 , out of the $|\mathcal{X}|$ possible x_2 candidates,

the best x_2 minimizing equation (8) is selected and then the same operation is repeated for last layer x_1 where we find best x_1 for each of the $|\mathcal{X}|$ surviving hypothesis of (x_3, x_2) pairs.

A. Spatial Trellis Interpretation

ML detection corresponds to sequence estimation over a spatial ISI channel. Each layer represents a decoding stage, and nodes represent constellation hypotheses. The ML path emerges only after full trellis depth is explored; early pruning may eliminate the correct path.

Equations (7) to (9) are similar to a 3-tap ISI channel as given below

$$\begin{aligned} y_0 &= h_0 x_0 \\ y_1 &= h_0 x_1 + h_1 x_0 \\ y_2 &= h_0 x_2 + h_1 x_1 + h_2 x_0 \end{aligned} \quad (9)$$

and hence reveal a *causal spatial ISI structure*:

- Symbol x_3 interferes with observations of x_2 and x_1
- Symbol x_2 interferes with observations of x_1
- Only x_1 is interference-free at full depth

Thus, MIMO detection after QR decomposition is equivalent to sequence estimation over a spatial ISI channel, where the “time” axis corresponds to the decoding order.

1) *Implication for Detection Algorithms*: The spatial ISI interpretation implies that:

- ML detection is a *sequence estimation* problem, not independent symbol slicing
- Early pruning (e.g., sphere decoding) may eliminate the true ML path prematurely
- Retaining competing hypotheses until sufficient depth is essential
- Multiple decoding orders correspond to multiple spatial trellises

This perspective naturally motivates reduced-complexity, list-based, and multi-order detection strategies that preserve ML hard decisions while significantly reducing computational complexity.

Define branch metrics:

$$BM_3(x_3) = |y_3 - r_{33}x_3|^2 \quad (10)$$

$$BM_2(x_2, x_3) = |y_2 - r_{22}x_2 - r_{23}x_3|^2 \quad (11)$$

$$BM_1(x_1, x_2, x_3) = |y_1 - r_{11}x_1 - r_{12}x_2 - r_{13}x_3|^2 \quad (12)$$

Path metric at depth k:

$$PM_k = \sum_{i=3}^k BM_i \quad (13)$$

In fig. (1), in stage 1, there are $|\mathcal{X}|$ nodes and BM_3 is computed for each. At Stage 2, for each x_3 hypothesis, x_2 for all possible $|\mathcal{X}|$ candidate values are evaluated. The x_2 minimizing $BM_2(x_2, x_3)$ is retained per x_3 , resulting in $|\mathcal{X}|$ surviving (x_3, x_2) hypotheses. This is mathematically equivalent to finding x_2 using equation 11 for the given x_3 . This conditional minimization does not collapse the trellis and preserves multiple hypothesis for subsequent stages. PM metric is also computed for the $|\mathcal{X}|(x_3, x_2)$ pairs. And this is repeated till the final stage. This is where the multiple

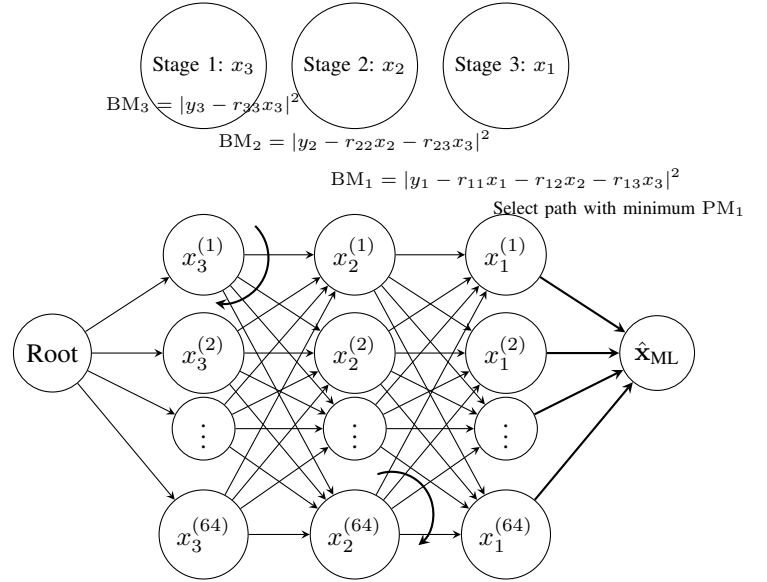


Fig. 1: Spatial Trellis Interpretation of 3x3 MIMO (64QAM). Arc represents select min (survivor) out of $|\mathcal{X}|$ outgoing paths

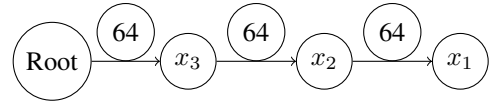


Fig. 2: Multi-Pivot in 3x3 MIMO 64QAM: Search one pivot on x_3

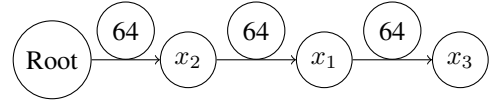


Fig. 3: Multi-Pivot in 3x3 MIMO 64QAM: Search two pivot on x_2

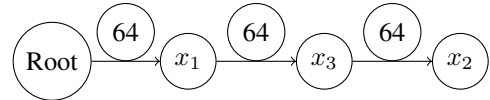


Fig. 4: Multi-Pivot in 3x3 MIMO 64QAM: Search three pivoting on x_1

hypothesis and trellis (MHT) part of MT-MHT-MD comes from.

The above figure further illustrates the proposed interpretation of ML MIMO detection as a spatial trellis traversal problem. Each decoding order induces a distinct trellis, where all constellation hypotheses are retained at each depth. Crucially, the correct ML path does not dominate until full depth due to residual inter-layer interference, motivating delayed pruning.

ML MIMO detection can be viewed as sequence estimation over a spatial ISI channel. Different column permutations of the channel matrix induce different spatial trellises. While all trellises correspond to the same ML objective, their intermediate metrics evolve differently. Retaining all constellation hypotheses until sufficient trellis depth ensures that the true ML path is not prematurely eliminated. This is where the Multi-Pivot (MP) part of MP-MHT-MD comes from. By virtue of this multi-pivot construction, competitor bit is always

assured for soft llr computation.

The proposed algorithm may be interpreted as reverse-viterbi in the sense the pruning happens on the possible outgoing paths for each of the nodes at any stage k , $k = N_t - 1, N_t - 2, \dots, 1$.

For 2×2 , the 2 pivots with full hypotheses are as follows. It can be inferred that the $2|\mathcal{X}|$ list obtained this way actually contains the ML and the closest competitor pair for all bits in terms of euclidean distance as in the ML solution of size $|\mathcal{X}|^2$ and hence the soft/hard decisions are ML optimal (in max log sense) [1][2].

For $N_t \times N_t$, the solution is very close to hard ML and the soft llrs are also guaranteed for all bits because of the multi-pivot, multi-hypothesis approach. But they are over-estimated because the closest competitor bit/symbol pair is not guaranteed to be in the $N_t|\mathcal{X}|$ list. However forward error correction algorithms such as ldpc/turbo may tolerate the over-estimated llrs.

Figure 1 may also be interpreted as a classical ML sequence estimation (MLSE) problem over an equivalent spatial ISI channel with slight modification. In this interpretation, all candidate symbols at Stage 1 are considered and the branch metric BM_3 is computed. For each node at Stage 2, the best incoming path is then retained by minimizing the accumulated metric $BM_2 + BM_3$, analogous to conventional Viterbi decoding. The same procedure is repeated at Stage 3 to obtain the final ML solution. However, this formulation requires evaluating $|\mathcal{X}|^2$ metrics per stage, resulting in a complexity that scales quadratically with the constellation size for any MIMO configuration. When extended to a multi-pivot formulation, the overall complexity increases to $N_t|\mathcal{X}|^2$, which remains significantly higher than that of the proposed detector. In contrast, the proposed algorithm exploits the upper-triangular structure obtained from QR decomposition, together with Viterbi-like pruning, to achieve a substantially lower and deterministic complexity.

B. Algorithm

The proposed algorithm is illustrated in Algorithm 1 section below. Please note that step 11 in the algorithm is effectively same as solving for x_k using the equation corresponding to that layer after doing QR application (as illustrated by step 12).

IV. RESULTS

Simulations were run in a simplified framework with independent and identically distributed (iid) rayleigh channel with QPSK, 16-QAM, 64-QAM and 256-QAM for 2×2 , 3×3 , 4×4 , 6×6 and 8×8 without any error control coding. Brute-force ML, proposed method with different list sizes and QR-ZF are simulated and BER vs SNR is plotted for each method.

V. KEY OBSERVATIONS AND INSIGHTS

- For 2×2 MIMO, the proposed method is exactly same as ML in hard decision and soft-llrs in max log sense but with list size of only $2|\mathcal{X}|$ corresponding to ordering of (x_1, x_2) and (x_2, x_1) .

Algorithm 1 Multi-Pivot Multiple-Hypothesis Trellis-Based MIMO Detection

Require: Received vector \mathbf{y} , channel matrix \mathbf{H} , constellation \mathcal{X} , noise variance σ^2

Ensure: Hard ML estimate $\hat{\mathbf{x}}$, soft LLRs

- 1: Initialize candidate list $\mathcal{L} \leftarrow \emptyset$
- 2: **for** each pivot layer $p \in \{N, N-1, \dots, 1\}$ **do**
- 3: Reorder columns of \mathbf{H} such that symbol x_p is the **first enumerated layer**
- 4: Perform QR decomposition to obtain \mathbf{R} and transformed \mathbf{y}
 {Stage 1: enumerate pivot-layer hypotheses}
- 5: **for** each $x_p \in \mathcal{X}$ **do**
- 6: Compute branch metric:

$$BM_p(x_p) = |y_p - r_{pp}x_p|^2$$

- 7: Initialize path (x_p) with $PM_p = BM_p(x_p)$
- 8: **end for**
 {Stages 2 to p : conditional best-symbol selection}
- 9: **for** $k = p-1$ down to 1 **do**
- 10: **for** each retained hypothesis path **do**
- 11: For all $x_k \in \mathcal{X}$, compute the conditional branch metric and select:

$$BM_k(x_k) = \left| y_k - \sum_{j=k}^p r_{kj}x_j \right|^2, \hat{x}_k = \arg \min_{x_k \in \mathcal{X}} BM_k(x_k)$$

- 12: OR equivalently compute (instead of step 11):

$$\hat{x}_k = \text{slice}\left(\left(y_k - \sum_{j=k+1}^p r_{kj}x_j\right)/r_{kk}\right)$$

- (only the selected symbol \hat{x}_k is retained; no alternative hypotheses are expanded at this stage.)
- 13: Update path metric:

$$PM_k = PM_{k+1} + BM_k(\hat{x}_k)$$

- 14: **end for**
- 15: **end for**
- 16: Store all completed paths (\mathbf{x}, PM_1) in \mathcal{L}
- 17: **end for**
 {Final ML decision}
- 18: Select:

$$\hat{\mathbf{x}} = \arg \min_{\mathbf{x} \in \mathcal{L}} \|\mathbf{y} - \mathbf{R}\mathbf{x}\|^2$$

- {Soft-output computation}
- 19: **for** each layer k and bit position b **do**
- 20:

$$LLR_{k,b} = \min_{\mathbf{x}: b_k=1} \|\mathbf{y} - \mathbf{R}\mathbf{x}\|^2 - \min_{\mathbf{x}: b_k=0} \|\mathbf{y} - \mathbf{R}\mathbf{x}\|^2$$

- 21: **end for**
 - 22: **return** $\hat{\mathbf{x}}$, LLRs
-

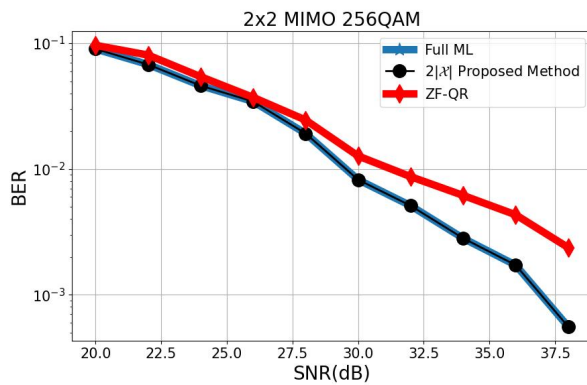


Fig. 5: BER performance for 2x2 MIMO 256QAM: Full ML vs Reduced-Search ($2|\mathcal{X}|$) vs ZF-QR

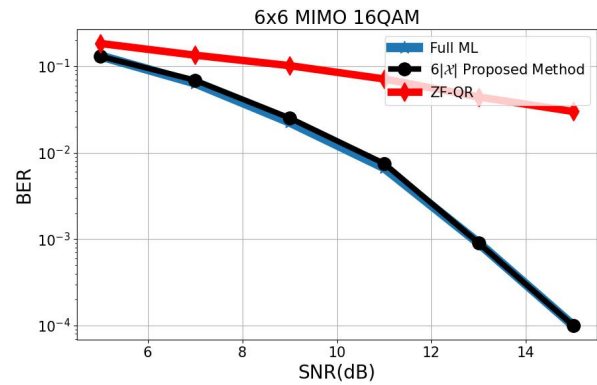


Fig. 8: BER performance for 6x6 MIMO 16-QAM: Full ML vs Reduced-Search ($6|\mathcal{X}|$)

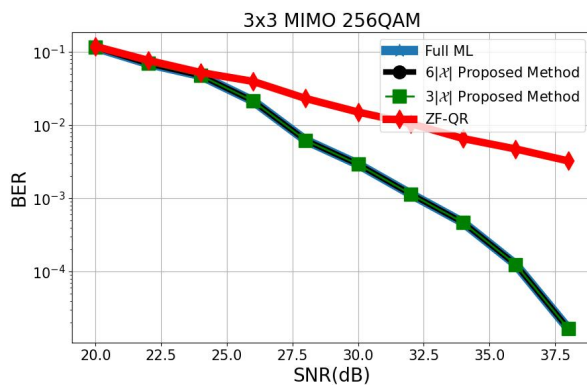


Fig. 6: BER performance for 3x3 MIMO 256QAM: Full ML vs Reduced-Search ($6|\mathcal{X}|$ and $3|\mathcal{X}|$) vs ZF-QR

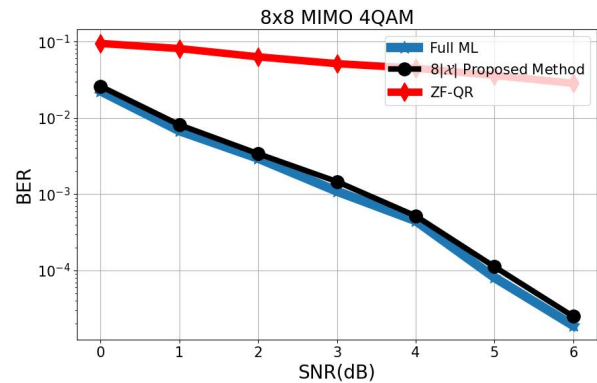


Fig. 9: BER performance for 8x8 MIMO QPSK: Full ML vs Reduced-Search ($8|\mathcal{X}|$)

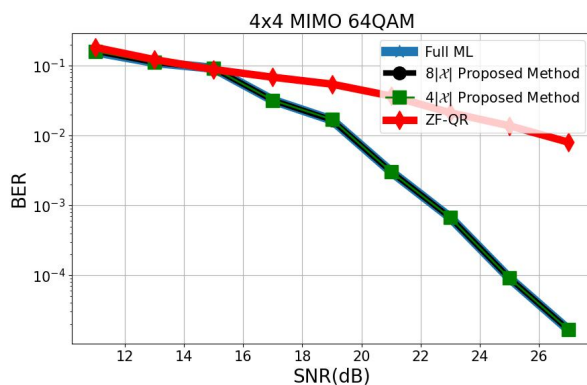


Fig. 7: BER performance for 4x4 MIMO 64-QAM: Full ML vs Reduced-Search ($8|\mathcal{X}|$ and $4|\mathcal{X}|$) vs ZF-QR

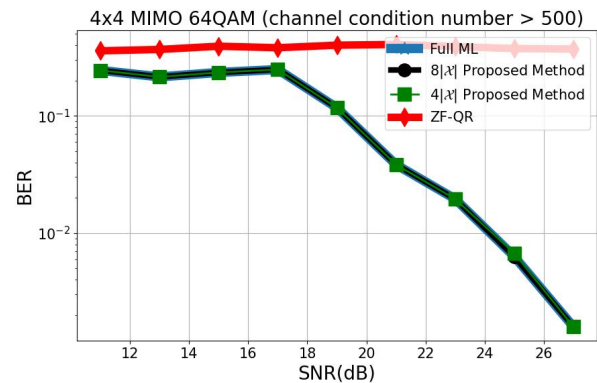


Fig. 10: BER performance for 4x4 MIMO 64QAM with channel condition number > 500 : Full ML vs Reduced-Search ($8|\mathcal{X}|$ and $4|\mathcal{X}|$) vs ZF-QR

- For 3×3 MIMO, the proposed method can be applied with $3! = 6$ times $|\mathcal{X}|$ list size or with $3|\mathcal{X}|$ list size. The former corresponds to ordering of (x_1, x_2, x_3) , (x_1, x_3, x_2) , (x_2, x_3, x_1) , (x_2, x_1, x_3) , (x_3, x_1, x_2) and (x_3, x_2, x_1) . The latter corresponds to some further simplifications to reduce complexity - the ordering being (x_1, x_2, x_3) , (x_2, x_3, x_1) and (x_3, x_1, x_2) .
- For upto 4×4 MIMO, there is no noticeable degradation in BER performance for the proposed methods compared to ML. For 6×6 MIMO and above, there is slight (still less than 0.1-0.2dB) degradation only.
- For $N_t \times N_t$ MIMO, the proposed method requires N_t pivots and can be applied with $N_t!|\mathcal{X}|$ list size (full hypothesis for all layers but with all combinations of other layers) or with much lesser complexity as $N_t|\mathcal{X}|$ list size (full hypothesis for each of the N_t layers)
- Reduced-search detection recovers ML-equivalent hard decisions across a wide range of SNRs, even under moderately ill-conditioned channel realizations.
- Dominant error events are driven by single-layer symbol deviations (though not shown here); multi-layer error events occur with significantly lower probability and contribute marginally to overall BER.
- High channel condition numbers increase noise enhancement but do not necessarily increase the dimensionality of dominant ML error events.
- The effective ML candidate set in practical fading channels grows approximately linearly with constellation size and number of transmit layers, despite exponential worst-case complexity.
- Competitors for calculating soft-output LLRs is always guaranteed because of the multi-pivot approach. For $> 2 \times 2$ configuration, soft-output LLRs may exhibit overconfidence due to reduced hypothesis enumeration especially in channels with high condition number; however, these errors are structured and can be mitigated via condition-number-aware scaling or LLR clipping.
- When combined with LDPC or Turbo decoding, the decoders may be able to tolerate moderate LLR overestimation and hence the proposed method can still achieve near-ML coded performance.
- If interference is present in the system, one can apply Interference Rejection Combining (IRC) followed by the proposed method resulting in reduced complexity IRC-ML. In addition, general pre-processing steps like lattice reduction can be performed before the proposed method is applied.
- Sphere decoding aggressively prunes early layers and risks discarding dominant ML competitors, whereas the proposed method retains full constellation hypotheses per layer, preserving ML-relevant candidates.
- The proposed detector exhibits deterministic and fixed complexity, in contrast to the highly variable and tail-dominated complexity of sphere decoding, enabling hardware-friendly real-time implementation, particularly on parallel architectures such as GPUs.

The trade-offs of the various detection algorithms are pre-

TABLE I: Comparison of MIMO Detection Algorithms

Comparison	ML	Proposed Method	Sphere Decoding
Performance	Optimal	Near-optimal	Near-optimal
Complexity	High (exponential)	Medium (linear in $ \mathcal{X} $)	Variable (polynomial on average)
Time Bound	Not practical	Deterministic	Not time-bounded
Soft-LLRs	Yes	Yes	Not guaranteed

sented in Table 1.

VI. LOOKING BACK

Although the QR-decomposed MIMO detection problem has long been recognized as algebraically equivalent to an ISI channel, this equivalence has typically been interpreted in a strict trellis sense, leading to the conclusion that Viterbi-style decoding would require a state space of size $|\mathcal{X}|^{N_t-1}$ and is therefore impractical. As a result, prior work has largely focused on sphere decoding and K-best algorithms that rely on early pruning and variable-complexity search.

In contrast, the present work revisits this equivalence by exploiting the causal, upper-triangular structure induced by QR decomposition. This structure ensures that, for a fixed hypothesis at a given layer, the optimal predecessor at the next layer is uniquely determined by metric minimization, thereby eliminating the need to retain multiple competing paths per node. This subtle but important distinction breaks the conventional ISI-trellis complexity barrier and enables a deterministic, reduced-search procedure that retains ML-like behavior while avoiding exponential growth in candidate paths. The resulting interpretation bridges classical MLSE intuition with practical MIMO detection and reveals complexity reductions that have not been explicitly identified in prior literature.

VII. SOFT-LLR RELIABILITY AND RANK-AWARE SCALING

While the proposed reduced-complexity detector achieves near-ML hard decision performance, the soft log-likelihood ratios (LLRs) obtained from a reduced candidate list may be over-estimated in certain scenarios, particularly when the closest competing hypothesis for a given bit lies far from the minimum-distance candidate in the reduced list. This behavior is inherent to any reduced-search detector and is not specific to the proposed approach.

To address this, a rank-aware LLR scaling mechanism is introduced that exploits the intrinsic geometry of the reduced search space without requiring any additional channel-dependent heuristics.

A. Soft LLR Computation from Reduced Candidate List

Let $\mathcal{C} = \{\mathbf{x}_k\}_{k=1}^{N_c}$ denote the reduced candidate list generated by the proposed detector, with corresponding Euclidean distance metrics $\{d_k\}_{k=1}^{N_c}$, sorted such that

$$d_{(1)} \leq d_{(2)} \leq \dots \leq d_{(N_c)}. \quad (14)$$

For stream t and bit position b , the soft LLR is computed as

$$\text{LLR}_{t,b} = d_1 - d_0, \quad (15)$$

where

$$d_0 = \min_{k:b_{t,b}(\mathbf{x}_k)=0} d_k, \quad (16)$$

$$d_1 = \min_{k:b_{t,b}(\mathbf{x}_k)=1} d_k. \quad (17)$$

B. Rank-Based Confidence Measure

Let $r_{t,b}$ denote the rank position (in the sorted metric list) of the closest competing hypothesis for bit (t, b) , i.e., the candidate achieving $\min(d_0, d_1)$ corresponding to the opposite bit value of the ML decision. A normalized rank measure is defined as

$$\alpha_{t,b} = \frac{r_{t,b} - 1}{N_c - 1}, \quad \alpha_{t,b} \in [0, 1]. \quad (18)$$

A small value of $\alpha_{t,b}$ indicates that the closest competing hypothesis is near the ML candidate and the corresponding LLR is reliable, whereas larger values indicate weaker competition and potential over-confidence.

C. Rank-Aware LLR Scaling

The final scaled LLR is obtained as

$$\text{LLR}_{t,b}^{\text{scaled}} = \text{LLR}_{t,b} \cdot g(\alpha_{t,b}), \quad (19)$$

where $g(\cdot)$ is a monotonic decreasing scaling function.

Two practical choices are considered:

1) *Linear Scaling*:

$$g(\alpha) = 1 - \beta\alpha, \quad (20)$$

where $\beta \in [0, 1]$ controls the aggressiveness of the scaling.

2) *Exponential Scaling*:

$$g(\alpha) = \exp(-\gamma\alpha), \quad (21)$$

where $\gamma > 0$ determines the decay rate.

Both forms preserve LLR magnitude when the competing hypothesis is close to the ML candidate and progressively reduce over-confidence when the competitor appears deeper in the reduced list.

D. Discussion

The proposed rank-aware scaling leverages information already available from the reduced-search detector and introduces negligible additional complexity. Unlike channel-condition-number-based scaling methods, the proposed approach adapts on a per-bit basis and directly reflects the geometry of the reduced ML search space. Simulation results indicate that this scaling improves soft-decoding robustness when combined with LDPC or turbo decoders, while preserving near-ML hard decision performance.

VIII. FURTHER WORK

Several directions for future research remain open. Lattice-reduction-based preprocessing may be combined with the proposed detection framework to further improve robustness in highly spatially correlated or ill-conditioned channels. The current study focuses on single-user MIMO scenarios with identical constellations across all spatial layers. An important extension is the evaluation of the proposed algorithm in multi-user MIMO (MU-MIMO) and heterogeneous SU-MIMO settings, where different users or layers may employ distinct modulation and coding schemes. Some optimizations/list size reductions when precoding is employed (or in general) can also be explored. Condition number based switching between ZF/MMSE and the proposed method is another area. Finally, the broader applicability of the proposed multi-pivot, multiple-hypothesis search framework to lattice problems beyond MIMO detection—such as the Closest Vector Problem (CVP)—is a promising direction for further exploration.

IX. CONCLUSIONS

The proposed method effectively bridges the performance gap with respect to ML but at significantly lower complexity, even though exact ML remains computationally intractable.

This work demonstrates that:

- Exponential ML complexity is unnecessary in practical MIMO systems
- Near-ML hard and soft decisions are achievable with linear list sizes
- The approach scales cleanly from 2×2 to 8×8 MIMO

The author hopes that the insights and interpretations presented in this work will be of interest to both industry and academia, and may stimulate further investigation into related detection, inference, and lattice-search problems.

REFERENCES

- [1] Logeshwaran Vijayan, Partha Sarathy Murali, Sundaram Vanka, "Reduced complexity maximum likelihood decoder for MIMO communications", Patent US7965782B1, June 21, 2011.
- [2] M. Siti and M. P. Fitz, "A Novel Soft-Output Layered Orthogonal Lattice Detector for Multiple Antenna Communications," 2006 IEEE International Conference on Communications, Istanbul, Turkey, 2006, pp. 1686-1691, doi: 10.1109/ICC.2006.254962.